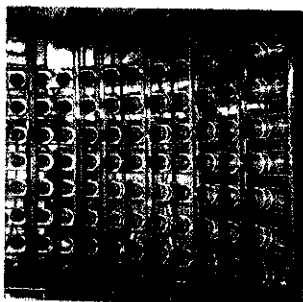
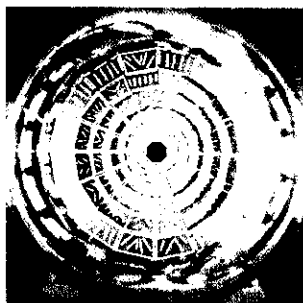


LABORATOIRE DE PHYSIQUE CORPUSCULAIRE



SUPER-HEAVY NUCLEI PRODUCTION AT GANIL

J. Péter, N. Alamanos, N. Amar, J.C. Angélique, R. Anne, G. Auger, F. Becker, R. Dayras, A. Drouart, J.M. Fontbonne, A. Gillibert, S. Grévy, D. Guerreau, F. Hanappe, R. Hue, A.S. Lalleman, N. Lecesne, T. Legou, M. Lewitowicz, R. Lichtenthaler, E. Liénard, W. Mittig, F. De Oliveira, N. Orr, G. Politi, Z. Sosin, M.G. Saint-Laurent, J.C. Steckmeyer, C. Stodel, J. Tillier, R. De Turreil, A.C.C. Villari, J.P. Wieleczko, A. Wieloch.
FULIS Collaboration

Novembre 2001

LPCC 01-13

Paper presented at International Symposium on Exotic Nuclei
EXON 2001, Baikal Lake, Russie, 24-28 July 2001

CENTRE NATIONAL DE LA RECHERCHE SCIENTIFIQUE

INSTITUT NATIONAL
DE PHYSIQUE NUCLÉAIRE ET DE PHYSIQUE DES PARTICULES

INSTITUT DES SCIENCES DE LA MATIÈRE ET DU RAYONNEMENT

UNIVERSITÉ DE CAEN

- U.M.R.6534 -

ISMRA - 6, Boulevard Maréchal Juin - 14050 CAEN CEDEX - FRANCE

Téléphone : 02 31 45 25 00 - Télécopie : 02 31 45 25 49
Internet : <http://www.cea.fr>

CERN LIBRARIES, GENEVA



CH-P00038467

SUPER-HEAVY NUCLEI PRODUCTION AT GANIL

J. PÉTER¹ AND THE FULIS COLLABORATION: N. ALAMANOS³, N. AMAR¹,
 J.C. ANGÉLIQUE¹, R. ANNE², G. AUGER², F. BECKER², R. DAYRAS³,
 A. DROUART³, J.M. FONTBONNE¹, A. GILLIBERT³, S. GRÉVY¹, D. GUERREAU²,
 F. HANAPPE¹, R. HUE², A.S. LALLEMAN², N. LECESNE², T. LEGOU¹,
 M. LEWITOWICZ², R. LICHTENTHÄLER⁴, E. LIÉNARD¹, W. MITTIG²,
 F. DE OLIVEIRA², N. ORR¹, G. POLITI⁵, Z. SOSIN⁶, M.G. SAINT-LAURENT²,
 J.C. STECKMEYER¹, C. STODEL², J. TILLIER¹, R. DE TOURREIL², A.C.C. VILLARI²,
 J.P. WIELECZKO², A. WIELOCH⁶

1 : LPC, Université and ISMRA, Caen, France, 2 : GANIL, Caen France,
 3 : DAPNIA/SPhN, C.E.N. Saclay, France 4 : I.F.U.S.P., São Paulo, Brazil
 5 : Università di Catania, Italy 6 : Ins. Fyziki Uniw., Krakow, Poland

1 Introduction

A programme on the study of super-heavy nuclei was started at GANIL since the performances of the accelerator and of the velocity filter LISE3 provided us with the necessary tools. First, a high beam intensity. Since the cross sections are very low, it is necessary to use large beam intensities, at least one particle- μA ($6.27 \cdot 10^{12}$ projectiles/s). Such intensities are produced by ECR sources. Second, the Wien filter LISE3, which had been built for improving the separation of isotopes performed by the spectrometer LISE, is powerful enough to separate the projectiles from the complete fusion evaporation residues emitted near 0 degree. The experimental set-up is described and the performances reached on known isotopes are given in the second and third parts, respectively. Beams of ^{84}Se and ^{76}Ge make it possible to directly form via cold fusion isotopes of elements $Z=108$ to 115 or 113, respectively, which have two more neutrons than the isotopes formed via cold fusion with ^{208}Pb or ^{209}Bi [1]. These possibilities were discussed in previous talks [2, 3]. The assets of inverse kinematics are shown in the fourth part and plans for experiments with lead beams are described in the fifth part. The plans of other groups for studying the structure and reactions of super-heavy nuclei at GANIL are briefly described in the last part.

2 Experimental set-up.

A complete set-up has been built and tested (see figure). The Wien filter LISE3 has crossed magnetic and electric fields at the same location rather than successive fields, which helps to reduce the background due to scattered projectiles. It is

divided into two identical halves and followed by a dipole magnet. It had been designed for the purification of exotic secondary beams produced by fragmentation in the LISE magnetic device and several modifications were found to be necessary for the study of complete fusion evaporation residues (ER's) and the rejection of the primary beam : - a reaction chamber was added just before LISE3, - the upper plate in the first half of the filter was moved up, the beam is thus deflected after this first half without hitting the plate and stopped on a water-cooled plate - two pairs of independently movable slits

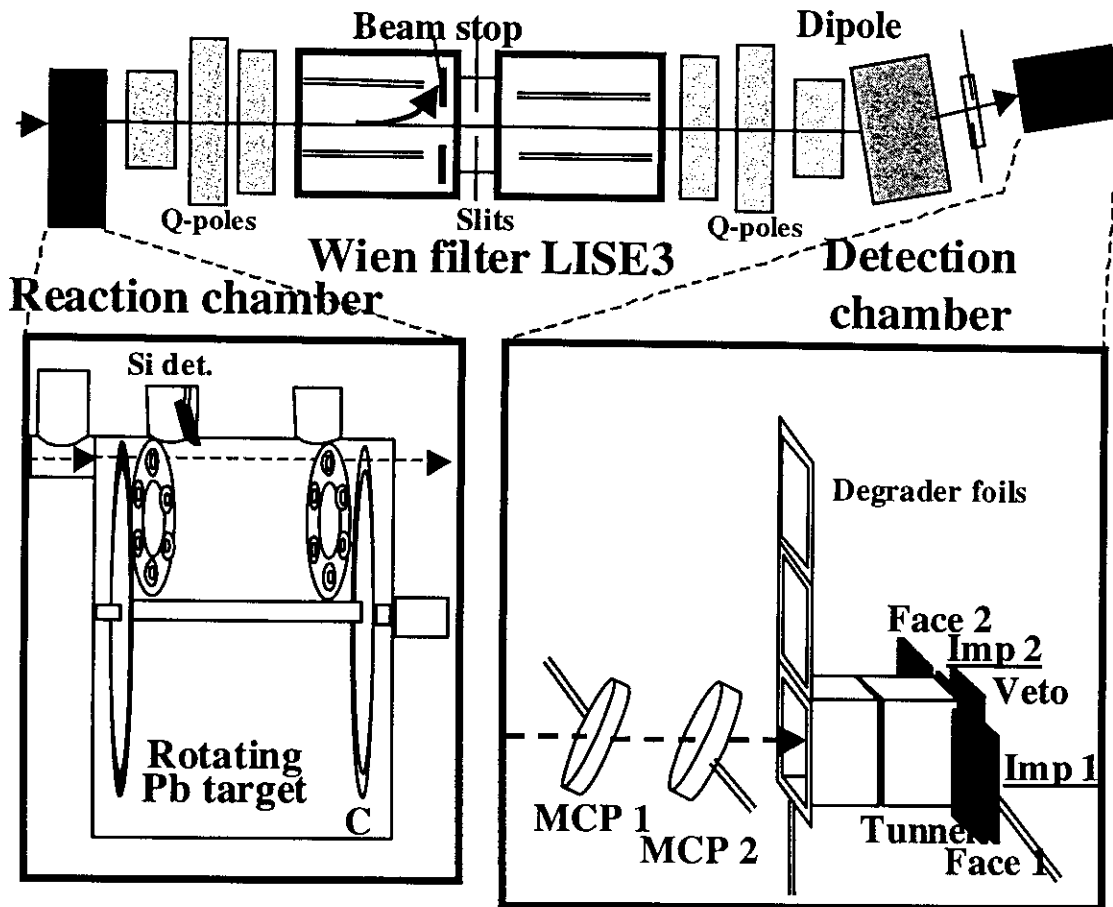


Figure 1 –Experimental set-up

and a beam profiler were installed at mid-filter. The suppression of unwanted products is improved by a dipole magnet located after the velocity filter.

The reaction chamber contains a wheel bearing 35 targets on a diameter of 670 mm and rotating at 2000 RPM, allowing targets with a low melting temperature (Pb, Bi) to sustain intense beams. The time structure of the beam is synchronised with the rotation. Smaller rotating targets are used for targets having a higher melting temperature. A Si detector continuously monitors the status of each target.

The velocity of each product is obtained with 2 aluminised mylar foils and micro-channel plate detectors; its kinetic energy and localisation are given by a X-Y Si implantation detector (Imp1 or 2). The energy of α -particles and fission fragments escaping from Imp is measured with a "tunnel" of 8 Si detectors. A Si veto detector is installed behind Imp to reject light particles which might punch through it. When emission of α -particles or fission fragment in Imp1 is identified via electronics, the beam is immediately stopped for a short while, during which Imp1 is moved out and Imp2 comes in; then the beam is sent again. α -particles escaping from Imp1 are then detected by the Si detector Face1. It is thus possible to study α -emission or spontaneous fission on long durations without any background. Specific electronics and data acquisition systems were developed. A fast analysis program allows us to identify α -decay chains or spontaneous fission on line.

The transmission of fusion nuclei from the target position through the quadrupoles, filter and final dipole was studied via a simulation code. The optics was checked and the Wien filter was calibrated using low energy (0.35 MeV/u) ions. The response of the whole set-up was checked via complete fusion reactions with known cross sections and α decay chains: $^{204-206}\text{Fr}$ nuclei formed via $^{86}\text{Kr} + \text{natSb}$ fusion reactions with cross sections of 10 to 300 μb [4], $^{260,261}\text{Sg}_{106}$ nuclei formed via $^{54}\text{Cr} + ^{208}\text{Pb}$ with cross sections of 300-500 pb [1].

3 Experiments.

3.1 Studies with $^{260,261}\text{Sg}$

With the Pb targets and a ^{54}Cr beam of 40nAp, the silicon implantation detectors measured a counting rate of 5-10 Hz. 2 different energies were used : 4.698 and 4.756 MeV/u. The excitation energies correspond mostly to the 1 neutron evaporation channel ($^{261}\text{Sg}_{105}$, cross section peaking at 500 pb) and to the tail of the 2 n excitation function [1].

With the on-line analysis, we indeed observed 2 decay chains of ^{261}Sg at 4.698 MeV/u whereas at 4.756 MeV/u we observed 9 chains with the characteristics (lifetimes and α energies) attributed to ^{261}Sg and 1 event attributed to ^{260}Sg (spontaneous fission). The decay chains were identified by position correlation in the Si detector between the implantation of the evaporation residue ER and the decay by α emission or fission. A transmission efficiency above 60 % and a suppression factor of the primary beam of $2 \cdot 10^{10}$ were achieved.

3.2 Search for element 118.

In 1999 ^{86}Kr on ^{208}Pb studied at Berkeley produced 3 events with a chain of 6 α 's which were attributed to element 118 and its descendants, with a cross section ~ 2.2

pb [5]. The same system studied with the velocity filter SHIP in Darmstadt did not lead to the observation of any event attributable to element 118, with an upper limit of 1 pb [6]. Since Ganil is able to deliver a high intensity beam of ^{86}Kr (15 μA with charge 10+, i.e. nearly 10^{13} projectiles/s) it was decided to try to obtain additional information: i) possible α decay before the minimum time of 120 μs in the Berkeley experiment. This required a faster acquisition system. ii) detection of α emitted more than 1 mn after implantation of the ER: the movable implantation detector described in the previous section was installed. iii) ER's may be created in an isomeric state which decays via electron capture followed by an electron cascade with an unknown half-life, modifying the ionic charge and strongly reducing the transmission. The carbon stripper foil which re-establishes the ionic charge distribution was located 3 times further, i.e. at larger times, than in the SHIP experiment.

With a total dose of 1.1×10^{18} ions at 5.27 MeV/u no event attributable to a super-heavy nucleus was observed. A similar result was obtained also at RIKEN [7] and very recently the identification of element 118 was cancelled by the Berkeley group [8].

4 Assets of inverse kinematics.

Inverse kinematics has an obvious drawback relative to usual kinematics: the velocity difference between the beam and the evaporation residues is much smaller so that larger magnetic and electric fields are necessary in a velocity filter. LISE3 is powerful enough to obtain the same separation at mid-filter (fig. 1). Another difficulty is the larger energy deposit in the target and the stripper foil. This increases the heating of the targets, but they usually have higher melting temperatures than Pb or Bi. A more serious problem is the increase in mechanical effects: the formation of micro-holes becomes more important.

There are however several assets. They concern the quality of the data as well as the duration of the experiment.

The first gains concern the beam time:

- the target thickness is no longer limited by multiple scattering of the ER's in the target. Therefore, instead of covering only 3-4 MeV in excitation energy, a target thick enough to cover the whole excitation function of interest may be used: 8 to 12 MeV, thereby maximising the counting rate. The most important application is the search for an unknown element. Indeed in cold fission, the maximum of the 1n excitation function is located at an excitation energy equals to the sum of the neutron separation energy $S_n(Z,A)$, the average energy of this neutron (twice the temperature, i.e. ~ 1 MeV here) and the fission barrier of the ER, $B_f(Z,A-1)$. As seen in table 1 for element 114, different mass tables lead to an uncertainty of several MeV on the mass balance Q , i.e. on the excitation energy for a fixed incident energy. There is also an uncertainty on S_n . In this example the uncertainty due to Q

and Sn is 4.6 MeV in c.m. . In addition, predictions on the value of Bf differ by several MeV : for $^{283}114$, it is 6-8 MeV in [9] and 2.4 MeV in [10]. In hot fusion, similar uncertainties are present. For covering the overall uncertainty on the incident energy of ~10 MeV in direct kinematics, lengthy measurements at several incident energies must be made [1]. In inverse kinematics, only one measurement will be necessary.



Table	M CN	- Q exp+tab	- Q table	Sn	Q + Sn +1 MeV
MySw 94 [25]	166,75	261,73	261,12	7,89	270,62
MoNiMySw 95 [26]	165,28	260,26	260,03	7,79	269,05
MaPeRaTo 98 [27]	167,01	261,99	262,75	8,55	271,54
KoUnTaYa 00 [28]	169,86	264,84	264,92	7,85	273,69
LiMaZe 01 [29]	169,99	264,97		7,22	273,19

Table 1 – Calculation of the location of the 1n excitation function according to several recent mass tables. Successively: reference of mass tables • predicted mass defect of the compound nucleus • mass balance using the experimental masses of the projectile and target • mass balance with all masses taken from the table • neutron separation energy Sn • c. m. energy corresponding to the threshold of 1 neutron evaporation. In each column, the minimum and maximum values are in bold characters. For locating the maximum of the excitation function, the fission barrier value of the ER must be added; its uncertainty is also of several MeV (see text).

- the strong forward focussing of ER's ensures a better transmission, even after α -decay in flight, whereas the transmission is reduced by a factor 2 to 3 in direct kinematics.

- the mean value of the ionic charge distribution of ER's is better known and the width of this distribution relative to the mean value is smaller, thereby improving the transmission.

The other gains concern the quality of the data:

- the energy deposited by an implanted ER is large and measured with a much better accuracy so that it is able to provide, combined with the time-of-flight, an estimate of the ER mass. This is valuable additional information

- the ER's penetrate more deeply in the implantation detector. If spontaneous fission occurs, both fission fragments are stopped in this detector and the fission total kinetic energy is easily and accurately measured. On the contrary, in direct kinematics one fragment leave a part of its energy in the entrance windows of the implantation detector and one of the tunnel detectors, so that the TKE of each event is affected by a different loss. α -particles emitted backwards leave at least 2 MeV in this detector and cannot be missed, while in direct kinematics some of them leave a very small and ambiguous signal.

This method is suitable for all aspects of super-heavy nuclei studies and can be applied to all systems, in hot, "warm" or cold fusion reactions.

5 Plans with lead beams.

We will first use this method with reactions which were found to have the largest cross sections up to $Z=112$: cold fusion of ^{208}Pb with neutron-rich isotopes [1]. In order to get new information on super-heavy nuclei, several systems, listed in table 2, can be studied for different purposes:

	Z	208Pb +...			207Pb+...		
		Tget	ACN	E*Bass	Tget	ACN	E*Bass
Rf	104	50Ti	258	23	50Ti	257	23
Db	105	51V	259	25	51V	258	25
Sg	106	54Cr	262	22	54Cr	261	22
Bh	107	55Mn	263	24	55Mn	262	24
Hs	108	58Fe	266	21	58Fe	265	20
Mt	109	59Co	267	23	59Co	266	22
	110	64Ni	272	17	64Ni	271	16
	111	65Cu	273	19	65Cu	272	18
	112	70Zn	278	12	70Zn	277	12
	113	71Ga	279	13	71Ga	278	13
	114	76Ge	284	9	76Ge	283	9
	115	75As	283	13	75As	282	13
	116	82Se	290	3	82Se	289	2
	117	81Br	289	7	81Br	288	6

Table 2 – Cold fusion reactions using lead isotopes 208 and 207. **In bold letters:** new reactions. Shaded areas: new paths to known isotopes. In frame: production of new isotopes via 1n and/or 2n channels.

5.1 *New paths to known isotopes with ^{208}Pb beams.*

The same compound nuclei and ER's with odd Z formed at GSI with a ^{209}Bi target ($Z=83$) and an even Z projectile can be formed with a ^{208}Pb beam ($Z=82$) and an odd-Z target. Two points are of interest:

1- to measure the cross section and to compare it to the known cross section with ^{209}Bi . That will give a clue to the respective roles of macroscopic and structure effects on the ER cross section: charge asymmetry of the entrance channel and closed shells in the partners. Indeed fusion with ^{208}Pb is less favoured due to the larger Coulomb repulsion (less asymmetric system than with ^{209}Bi) and larger excitation energy at the interaction barrier, but this may be partially compensated by its exactly filled shells. Theoretical calculations were made by several groups in order to reproduce the measured cross sections of ER's formed via cold fusion either with ^{208}Pb or with ^{209}Bi [11, 9, 12, 13, 14, 24]. Comparisons of cross sections of the same ER issued from the same compound nucleus formed by two different entrance channels will provide a sensitive check of the validity of these various approaches and add an additional constraint.

2- to reach different levels in the ER's, especially isomeric states indicated by an unusually large value of alpha-particle energies.

5.2 *Studies of Spontaneous Fission and α energies.*

For elements ranging from Fm to Rf ($Z=104$) the mass distributions of fission fragments are known to vary rapidly from symmetric to asymmetric shapes as a function of Z and A of the fissioning nucleus. The total kinetic energy (TKE) distributions also exhibit different shapes [15] and can be measured. As noted in section 4, in inverse kinematics the whole TKE is well measured in the implantation detector. Such studies will be made first on nuclei with a large spontaneous fission probability and not too low cross sections

5.3 *New isotopes formed with ^{207}Pb beams.*

Isotopes lighter by 1 neutron than the known isotopes of several elements can be produced with ^{207}Pb instead of ^{208}Pb : with ^{55}Mn the 2n channel leads to ^{260}Bh ($Z=107$) - with ^{59}Co , 1n : ^{265}Mt (109) - with ^{65}Cu , 1n : $^{271}\text{111}$ - with ^{70}Zn , 1n : $^{276}\text{112}$. For these last two cases, a chain of 3 α 's will be observed before reaching a known isotope, i.e. 3 new isotopes will be observed in one event.

$^{276}\text{112}$ offers the special interest of being an even-even nucleus. Its α decay and spontaneous fission are unhindered and can be more easily compared with theoretical predictions than nuclei with unpaired nucleon(s). In addition its level scheme is expected to be simpler.

This remark applies also to heavier elements. The heaviest stable isotope of target nuclei with $Z = 30$ to 44 (and more), has an even number of neutrons and the

isotope having only 1 neutron less does not exist. Therefore an even-N evaporation residue will be formed either with ^{208}Pb via radiative capture (0n, i.e. compound nuclei formed at excitation energies $< S_n$) or with ^{207}Pb via 1n evaporation if this channel remains favoured. Of course, ^{209}Pb projectiles radioactive beams will offer this same advantage as ^{207}Pb , and in addition will have larger cross sections. Their intensity might be sufficient since ^{209}Pb is obtained by transfer of 1 neutron only.

5.4 *New elements.*

Above $Z=109$, the counting rate is very low. For $^{277}\text{112}$ measurements were made at one beam energy only, which may not be at the maximum of the excitation function. Indeed the 1n excitation function seems to have its maximum shifted to smaller excitation energies with Z (due to the decrease in the fission barrier height) and also to become narrower [1]. The broad energy coverage provided by inverse kinematics may reveal a larger cross section value.

The 1n channel cross section decreases quickly with Z . It may be that the 0n cross section becomes larger than the 1n cross section, even though the fusion probability drops very much at the corresponding incident energy. Added to the uncertainty on the compound nucleus mass defect, the exploration of the broad range of incident energies corresponding to 0n+ 1n excitation functions leads to lengthy measurements at several incident energies in direct kinematics : 6 beam energies were tried for $^{82}\text{Se}+^{208}\text{Pb}$ reactions in a search for element 116 [1]. With a Pb beam, an excitation energy range of 12 MeV can be covered with a single incident energy.

5.5 *First experiments with Pb beams.*

The heaviest element for which the total kinetic energy distribution has been measured is Rf (104) [15]. A sufficient number of events was obtained for isotopes 258, 260 and 262. For isotope 256, few events were observed, making it possible to obtain only the average total kinetic energy. This isotope and the heavier element Sg (106) may be produced and studied in the same experiment. Indeed ^{208}Pb at 5 MeV/u on a ^{54}Cr target with a thickness of 0.6 mg/cm^2 make $^{262}\text{Sg}^*$ compound nuclei at excitation energies between 15 and 25 MeV : fig. 2. They de-excite mostly via evaporation of 2 neutrons, producing ^{260}Sg evaporation residues which decay via spontaneous fission with a partial width about 50 %. The other 50 % decay via α -emission to ^{256}Rf which decays almost totally via spontaneous fission. The average energy of ^{256}Rf will be compared to the literature value for calibration of the pulse height defect of fission fragments emitted within a Si detector. The TKE distributions of ^{256}Rf and ^{260}Sg will be obtained.

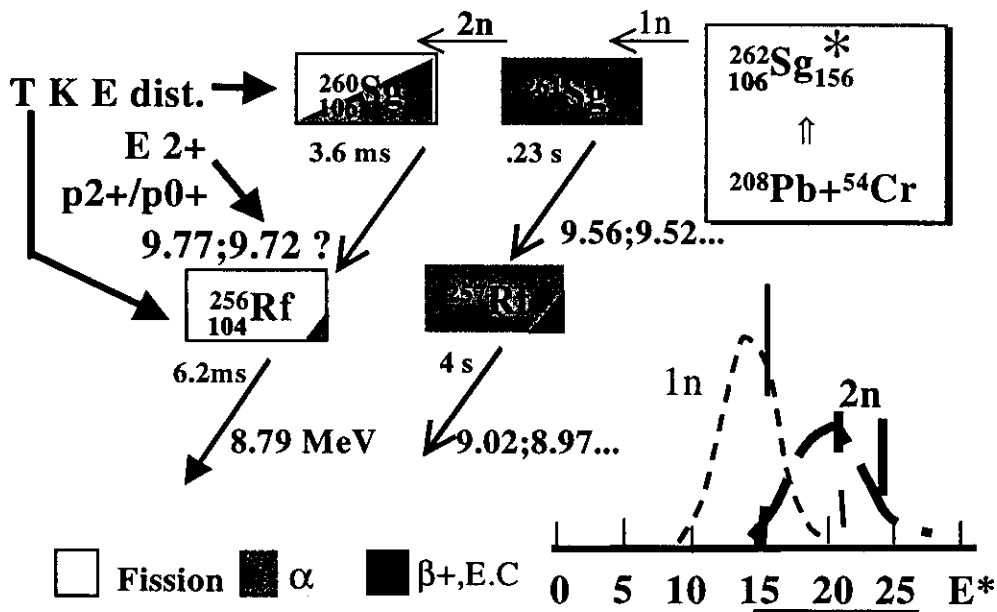


Fig. 2 - Reaction to be studied in order to get evidence for deformation of even-even super-heavy nuclei and to measure the Fission Total Kinetic Energy distribution of ^{260}Sg and ^{256}Rf

Also in the same experiment, the α decay of ^{260}Sg will offer information about an important characteristics of super-heavy nuclei around $Z=108$ and $N=162$. Theoretical analysis of the ground state energy and single-particle levels indicate that ^{270}Hs (108) is a doubly magic deformed nucleus: large quadrupole deformation. Experimentally these “deformed” nuclei were produced and observed, but there is no experimental evidence of their deformation. This evidence is necessary to establish that deformed nuclei may benefit from a strong shell structure which increases their fission half-life by several (or many) orders of magnitude, which makes it possible to detect them. Such an evidence can be found in observing a rotational band in the γ spectra. It was observed for nuclei as heavy as ^{254}No [16,17], but the smaller cross section of heavier elements does not allow us to use such a technique. Another method is to observe the first excited $2+$ state of an even-even isotope in the α -decay spectrum of its father nucleus: one should observe two peaks, corresponding to the decay to the g. s. and to the $2+$ level, respectively [18]. For very heavy nuclei (U to Fm), this level is calculated and observed to be around 45-50 keV. The calculated relative probability p_{2+}/p_{0+} of α -decay into this state and into the ground state, respectively, was also found to be in good agreement with the data. Therefore the calculated values for super-heavy nuclei are expected to be correct. For ^{256}Rf , the calculated values are: level = 43 keV and $p_{2+}/p_{0+} = 0.15$ [18]. An indication of such a level was found in the spectrum of 9 α -particles from ^{260}Sg [19]. It should be established on a larger statistics.

As shown in table 2, fusion of ^{208}Pb projectiles with ^{51}V will form the same odd-Z compound nucleus, ^{259}Db , and evaporation residues as the reaction $^{54}\text{Cr}+^{209}\text{Bi}$ for which the decay schemes and ER cross sections are known [1]. As noted in section 5-1, the comparison of the ER cross sections, 1n and 2n, between these two reactions will provide information on the factors favouring fusion and survival probability.

6 Structure and reaction studies.

Other groups made proposals for studying the structure of super-heavy nuclei at GANIL, and also for measuring reactions induced by these super-heavy nuclei. Of course, such studies require to choose nuclei produced in large numbers, i.e. $Z \geq 102$.

6.1 Structure studies

In order to get a better knowledge of the shell structure of SH nuclei, spectroscopic information should be obtained via various methods in addition to α -spectroscopy performed in the experiments described above (section 5-5 and figure 2): e- and γ -spectroscopy is being proposed by another group [20]. An important issue is the

location of the stabilizing spherical shell gap ($Z=114$ or 120 or 126 ?, $N=172$ or 184 ?) and the likely deformed sub-shells ($Z \sim 108$, $N \sim 152$).

Before reaching such nuclei, one should study trans-fermium nuclei similar to the heaviest nucleus studied yet via γ -spectroscopy: ^{254}No [16,17]. Not only these nuclei are produced with a much larger cross section, but also the orbitals involved in heavier SH nuclei are the ones which play a role for trans-fermium nuclei.

The goal of the experiment is to measure precisely the single-particle structure of ^{251}Md and ^{251}Fm . Little is known about ^{251}Md and does not fit with predictions. For ^{251}Fm two rotational bands were observed and two γ transitions were deduced. The assignment of the ground state spin and parity is tentative.

^{251}Md and ^{251}Fm will be produced via the reaction $^{48}\text{Ca}+^{209}\text{Bi} = ^{257}\text{Lr}$ followed by the evaporation of 2 neutrons, with a cross section of ~ 300 nb [21]. α -spectroscopy of ^{255}Lr will be performed and isomeric states will be looked for since they are present in this mass region and allows one to deduce the active orbitals. Most ^{255}Lr nuclei decay via α to ^{251}Md with a half-life of 21 s, and 90% of these ones decay via electron capture to ^{251}Fm . Since the ground state parity and the spin of the first level of ^{251}Fm are known, the ground state of ^{251}Md and possibly ^{255}Lr should be determined.

The experimental set-up will be similar to that of fig. 1. ^{255}Lr will be implanted in a X-Y Si detector, but the Tunnel will be made of Si detectors for electrons (and also α -particles). Indeed the expected low transition energies and the high Z value lead to

a rate of conversion-electrons higher than the rate for γ -rays. γ detectors for higher energies will be installed around the implantation detector: Ge detectors in the Clover geometry. A good point is that the electrons and γ -rays are emitted from nuclei at rest and do not suffer from the Doppler effect.

6.2 Reaction studies.

Another group intends to perform γ -ray spectroscopy of heavy nuclei following Coulomb excitation [22]. Even though Coulomb excitation has a large cross section, it will take several years before a sufficient number of SH nuclei can be produced, so these experiments will be applied first to transuranic nuclei. For the moment three points relate these experiments to the program of SH nuclei production : the method of production, the experimental set-up, indirect information on SH structure.

The nuclei will be produced in inverse kinematics at energies close to the fusion barrier: fusion of a ^{208}Pb beam at ~ 5 MeV/u and light nuclei. Among the assets of inverse kinematics (section 4), the main ones here are a better transmission through the spectrometers and the background reduction due to the long distance between the production area and the detection area. The first test will be made with ^{18}O target nuclei. The evaporation residues will be ^{222}Th which will be separated from the ^{208}Pb beam and Coulomb excited on a secondary target of Tin.

The set-up will be similar to fig. 1 with two important modifications. First, the primary target (^{18}O) will be installed ahead of the LISE magnetic spectrometer. Indeed the velocity difference between the projectile and the ER's is too small for allowing an efficient separation with the Wien filter LISE3 alone. Since the projectiles and ER's have different average ionic charges and velocities, their distributions of magnetic rigidities overlap only partially. Therefore a very large part of the projectile ionic charge distribution can be eliminated by LISE and the remaining part (about 10 %) will enter the Wien filter together with a large part of the ER's (about 60 %). Second, a secondary target, for Coulomb excitation, will be installed just before the detection area. The ER's will be identified by their characteristic α energies, or their well known γ 's for ^{222}Th

These data will provide the determination of nuclear states of the ER's and also $B(E2)$, $B(E3)$ values and hence deformations and lifetimes. Furthermore the systematic study of $B(E2)$ for heavy nuclei could give important information on the location of the spherical closure in super-heavy nuclei: $Z=114$ or 126 [23].

Acknowledgements

The authors want to thank all the technicians and engineers who made it possible to overcome the specific difficulties of these experiments: the electronics, detectors and mechanics groups at LPC Caen and Ganil, the data acquisition group GIP (Groupe d'Informatique Physique), the users support group (Service des aires) and the accelerator staff of Ganil for their continuous support and efficient performances

at all stages of this work. We are also indebted to the groups from CEN-Saclay for the fast conception and construction of the scattering chamber and rotating wheel: STCM (Service des Techniques de Cryogénie et Magnétisme) and SIG (Service d'Instrumentation Générale), and to the target laboratories of LNS Catania, IFU Sao Paulo, GSI Darmstadt and IPN Orsay for the excellent quality of their products, especially the large area lead targets.

References

- 1) S. Hofmann, G. Münzenberg, *Rev. Mod. Phys.* (2000)
- 2) C. Stodel et al., *Proc. Tours Symposium on Nuc. Phys.*, September 2000
- 3) J. Péter et al., *Proc. Int. Conf. Nuc. Phys. at Border Lines*, Lipari, May 2001
- 4) C.C. Sahm et al., *Nuc. Phys. A* **441**, 316 (1985)
- 5) V. Ninov et al., *Phys. Rev. Lett.* **83**, 104 (1999)
- 6) S. Hofmann, *Proc. Int. Conf. On Nuc. Phys.*, Sevilla (1999)
- 7) K. Morita, *comm. Int. Workshop on Fusion*, Dubna, May 2000, World Sci
- 8) K.E. Gregorich et al., *Phys. Rev. C* (to be submitted)
- 9) G. Giardina et al., *Eur. Phys. J. A* **8**, 205 (2000)
- 10) A. Mamdouh et al., *Nuc. Phys. A* **679**, 337 (2001)
- 11) G. G. Adamian et al., *Nuc. Phys. A* **633**, 409 (1998)
- 12) V. Yu. Denisov and S. Hofmann, *Phys. Rev. C* **61**, 034606 (2000)
- 13) Y. Aritomo., *Proc. Int. Workshop on Fusion*, Dubna, May 2000, World Sci
- 14) M. Ohta, *Proc. Int. Workshop on Fusion*, Dubna, May 2000, World Sci
- 15) D.C. Hoffman and M. R. Lane, *Rad. Chim. Acta* **70/71**, 135 (1995).
- 16) M. Leino et al., *Eur. Phys. J. A* **6**, 63 (1999)
- 17) P. Reiter et al., *Phys. Rev. Lett.* **82**, 509 (1999)
- 18) A. Sobiczewski et al., *Phys. Rev. C* **63**, 034306 (2001)
- 19) G. Münzenberg et al., *Z. Phys. A* **322**, 227 (1985)
- 20) Ch. Theisen et al., *Proposal for Ganil experiment E375* (2000)
- 21) H. W. Gäggeler et al., *Nuc. Phys. A* **502**, 561c (1989)
- 22) F. Hannachi et al., *Proposal for Ganil experiment E387* (2001)
- 23) N. V. Zamfir et al., *Phys. Lett. B* **357**, 515 (1995)
- 24) E.A. Cherepanov, *Pramana J. of Physics* **23**, 1(1999)
- 25) W.D. Myers and W.J. Swiatecki, *report LBL-36803, UC-413* (1994)
- 26) P. Möller et al., *At. Data Nucl. Data Tables* **59**, 185 (1995)
- 27) A. Mamdouh et al., *Nuc. Phys. A* **644**, 389 (1998)
and private communication
- 28) H. Koura et al., *Nuc. Phys. A* **74**, 47 (2000)
and report ISSN 1346-244X RIKEN-AF-NP-394
- 29) S. Liran et al., *At. Data Nucl. Data Tables* (2001)